IL NUOVO CIMENTO **41 C** (2018) 217
DOI 10.1393/ncc/i2018-18217-2

Colloquia: SIRR 2018

EURADOS Working Group 12 studies in interventional radiology for medical staff dosimetry

P. Ferrari([1])(*) E. Bakhanova([2]), F. Becker([3]), L. Campani([1]), V. Chumak([4]), J. Jansen([5]), Z. Jovanovic([6]), S. Khan([7]), D. Krstic([6]), F. Mariotti([1]), U. O'connor([8]), L. Pierotti([9]), S. Principi([10]), I. Clairand([11]) and Z. Knezevic([12])

([1]) *ENEA–IRP, Radiation Protection Institute Bologna - Bologna, Italy*
([2]) *National Research Center for Radiation Medicine - Kiev, Ukraine*
([3]) *Karlsruhe Institute of Technology - Karlsruhe, Germany*
([4]) *National Academy of Medical Sciences of Ukraine - Kiev, Ukraine*
([5]) *Public Health England - Chilton, Didcot, Oxfordshire, OX11 0RQ, UK*
([6]) *University of Kragujevac - Kragujevac, Serbia*
([7]) *Surrey University - Guildford, Surrey GU2 7XH, UK*
([8]) *St. James's Hospital - Dublin, Ireland*
([9]) *AOSP S.Orsola-Malpighi - Bologna, Italy*
([10]) *Universitat Politécnica de Catalunya - Barcelona, Spain*
([11]) *Institut de Radioprotection et de Sûreté Nucléaire - Fontenay-aux-Roses, France*
([12]) *Ruđer Bošković Institute - Zagreb, Croatia*

received 4 December 2018

Summary. — EURADOS (European Radiation Dosimetry Group) Working Group 12 (dosimetry in medical imaging) established a subtask devoted to the dosimetry of the medical staff employed in interventional radiology practices. As it is widely known, such practices are characterized by high doses, with respect the other medical procedures, both for the patient and the radiologist. For interventional cardiology there are several publications concerning medical staff dosimetry, on the contrary, for interventional radiology, data are more limited. For that reason WG-12 decided to study the irradiation scenario, employing simplified anthropomorphic models (MIRD type) with Monte Carlo simulations, reconstructing some specific interventional radiology practices (PTC and TIPS). In these procedures, where the X-ray C-arm is mainly fixed in PA projection and the beam directed to the patient abdomen, the radiologist is next to the patient right side, in correspondence to the

(*) Corresponding author. E-mail: paolo.ferrari@enea.it

liver region. The usage of the ceiling shielding is not very frequent, due to the difficulties in positioning it between the radiation source (the X-ray and the patient as the scattering source) and the operator. The aim of the simulations program is: to evaluate the dose received by the radiologist, in a region simulating the presence of the dosemeter fixed on the lead apron at the breast level; to estimate the corresponding effective dose; to make a sensitivity analysis on different parameters affecting the calculated results (as the reciprocal position between the two operators, the beam quality and the X-ray field dimension). Indeed a particular attention is devoted to the eye lens dosimetry, that has become a "critical issue" for personnel dosimetry, after ICRP has reconsidered the radiation sensitivity of the lens of the eye. In the present work the general scheme, the assumptions and the followed methodology are presented with some very preliminary results of the simulations and the measurements.

1. – Introduction

Interventional radiology and cardiology are widespread practices because they represent a minimally invasive valuable option for diagnosis and treatment of several pathologies (of heart, coronary and vascular system, biliary, esophagus, gastric and genitourinary system), for tumor therapy (embolization procedures) and pain management (vertebroplasty). These practices have large benefits for the patients, reducing hurt and avoiding the side effects of surgical treatments, but are known to increase the radiation exposure of patient and operators [1-4]. As a matter of fact, being fluoroscopy a guided procedure, the medical staff remains close to the patient during large part of the procedure and receives the radiation scattered by the patient itself [5-7]. In such context medical-staff radiation protection is a pivotal issue.

That scattered radiation is influenced by different factors such as the complexity of the procedure, the peculiarity of the case, the size of the patient, possible additional complications that extend the practice duration, the position and distances of the medical staff to the patient, the proper shielding and protective garments employment [8,9]. Some of these items are not controllable by the medical staff, instead others, such as the proper shielding usage, that could have a relevant impact on the radiation exposure, are [10,11]. In such context training and education can induce a better knowledge of the risk [12] by increasing the individual sensitivity to the radiation protection practice and leading to a better radiation dose awareness improving radiation safety.

With such intentions Working Group 12 (WG-12 dosimetry in medical imaging) has been established in EURADOS (European Radiation Dosimetry Group, `http://www.eurados.org/`). WG-12 activities have been aimed at patient and medical-staff radiation protection (with the exception of radiation therapy that is the focus of the EURADOS WG-9 group): skin dose measurement and dose alert thresholds in interventional practice [13-15]; eye lens dosimetry in interventional cardiology [16-20] and CT fluoroscopy [21].

The current WG-12 topics include, for patient dosimetry, skin dose mapping in clinical settings, reference levels for interventional cardiology and cone-beam CT dosimetry; whilst for medical-staff radiation protection, dosimetry of the lens of the eye (a crucial issue after the revision of its radiation sensitivity [22, 23]); a comparison of dosemeters

response calibrated in terms of $H_p(3)$; test active personal dosemeters, APD, usually employed in nuclear and industrial applications, in interventional radiology and cardiology room and a study of the exposure conditions of the physician in Percutaneous Transhepatic Cholangiography (PTC) and Transjugular Intrahepatic Portosystemic Shunt (TIPS), through Monte Carlo simulations, that is the subject of the present work.

In interventional radiology PTC is a quite frequent procedure, whilst TIPS is less frequent but is characterized by a higher dose to patient and medical staff, due to the longer fluoroscopy time. Considering the KAP-meter([1]) measurements and the fluroscopy time, $60\,\mathrm{Gy}\cdot\mathrm{cm}^2$ and 23 minutes can be reached for a biliary procedure *vs.* $446\,\mathrm{Gy}\cdot\mathrm{cm}^2$ and 115 minutes for TIPS (data taken from [24]). Notwithstanding the fact that these practices give lower radiation exposures to the medical staff with respect to interventional cardiology practices, being the radiologist really close to the patient abdomen, under which the X-ray source is placed, the doses received by the unprotected part of its body can be relevant [24] and this is particularly true when the ceiling shielding and the protective goggles are not properly used [25]. Taking into account the intrinsic variability of these procedures, numerical models and Monte Carlo simulations can supply important information on different parameters influencing the medical staff exposure. The aims of this study are therefore addressed to: evaluate the dose registered during the practice simulating the presence of a dosemeter fixed on the radiologist lead apron; determine the effective dose and doses to the lens of the eye and to the brain; perform a sensitivity analysis on different parameters affecting the calculated results (as the operators position, beam quality and X-ray field dimension); evaluate the effectiveness of the shielding in reducing the estimated doses. The study is just begun and will continue for several months. In the present paper the scheme, the main assumptions and the followed methodology are presented with some very preliminary results of the simulations compared to measurements and published data.

2. – Material and methods

2˙1. *The description of the irradiation scenario.* – The irradiation scenario is shown in fig. 1. The patient and the two operators are described through a modified version of the MIRD model [26] developed during the ORAMED project [8]. The MIRD model is based on the standard man description [27] and is 176 cm and 73 kg. During the ORAMED project, arms were modified and bent in order to better mimic their position in the interventional practice. In the present study the eyes were further modified, accordingly to a previous work [20], and a small volume, representing the eye lens, has been added inside the eye-ball. Indeed the operator brain (a simple ellipsoid) was subdivided into sections to better investigate the exposure condition of this organ. Tissue composition and densities have been taken from the ICRU report No.46 [28].

To reproduce the protective garment worn by the operators, a 0.5 mm lead apron and a thyroid collar were simulated. Contrary to what happens in interventional cardiology, in interventional radiology only few X-ray beam projections are used and generally

([1]) The KAP-meter is a transmission chamber installed on the X-ray tube exit on the C-arm used in the interventional practices to monitor the X-ray emission during the whole procedure. The measurements of the KAP-meter, expressed as the product by the kerma in air and the dimension of the fields, are normally used as a normalization factor to compare among practices and different measurements and can be employed as a first rough index of the dose received by the patient.

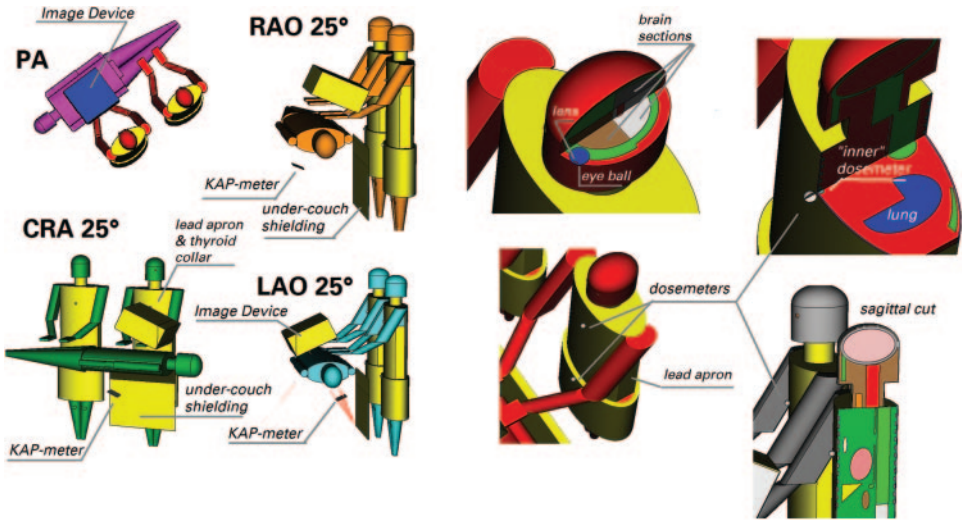

Fig. 1. – The X-ray beam projections and some cuts of the anthropomorphic models showing internal organs and tissues.

Postero-Anterior (PA) is predominant, if not unique, in many operations. However, for completeness and to compare outcomes with other studies, three additional X-ray beam projections were added: Right-Anterior Oblique 25°, RAO 25, Left-Anterior Oblique 25°, LAO 25, and Cranio-Caudal 25°, CRA 25. Only the lead shielding behind the patient couch is considered.

X-ray beam spectra where selected from the IPEM catalogue [29] and vary in terms of kV Al and Cu additional filtration. The X-ray beam is produced by a point source emitting a cone of photon, of fixed dimension, on the patient. In order to reproduce the square field of modern digital equipment, an ideal filter was inserted between the source and the simulated KAP-meter. The filter kills all the photons outside its central square aperture (*i.e.*, imp:p = 1 in the center and imp:p = 0 outside the aperture in MCNP syntax). The KAP-meter was designed as a simple thin volume of air between the source and the patient, rotating together with the source and the image device (a simple parallelepiped but shielded in order to absorb the leaking radiation). The source to the skin distance (SSD) was set to about 60 cm and the distance between the source and the image device (SID) was about 90 cm. These distances were kept constant for all irradiation conditions and are fairly representative of the routine practice. At the entrance of the image device, where the radiation exiting from the patient should be detected, a second thin air filler layer (called here IDEK: Image Device Entrance Kerma) is used for the normalization among projections. This should mimic the presence of the Automatic Exposure Control (AEC)([2]). The first operator is placed near the patient abdomen, with the hands almost in the X-ray field, a quite common situation in these

([2]) During the interventional practice, the Automatic Exposure Control (AEC) works to maximize the image quality and reduce the patient exposure: this implies that, depending on the projection (and on the absorption offered by the part of the patient traversed), the AEC controls the quantity of the photons emitted during the fluoroscopy and reaching the image device.

practices, and the second operator on its right (see fig. 1). To simulate the registered doses during medical-staff monitoring, a simplified dosimetric scoring volume was simulated as a small sphere (1 cm radius), filled by air, and positioned at the level of the breast of the operator, over the Pb apron. A second dosemeter was placed at the level of the waist. Both were put in on the sagittal mid-plane of the models, but a sensitivity analysis on their position is planned. Indeed, in order to simulate the response of a dosemeter positioned under the apron, an additional spherical volume, but filled by soft tissue, was cut inside the anthropomorphic model trunk, just below the skin, at 1 cm depth.

2˙2. *Scheme of the Monte Carlo simulations.* – The dosimetric study was divided into different tasks. For each task the different projections and the two operators are considered:

1) Doses to the operators: the scattered photon fluence entering the simulated dosemeter on apron is converted into $H_p(10)$ employing $\frac{H_p(10)}{\phi}$ conversion coefficients [30] (DE/DF card in MCNP syntax).

2) Protective garment: considering the absorbed dose inside and outside the apron it is possible to evaluate the efficiency of the protection supplied by the apron itself.

3) Eye lens doses: evaluate the doses to the lens of the eye lenses of the operator and compare the result with the dose received by the simulated dosemeter on the chest. This should allow to determine a sort of "dosimetric index" of the dose to the unprotected eye starting from the simulated measurement on the trunk.

4) "Male" effective dose: calculate the "male" effective dose for the two operators (they are both male) comparing it with the simulated $H_p(10)$.

5) Dose to the brain: evaluate the exposure of this organ and determine the corresponding "dosimetric index" as in the eye lens case.

These simulations have been performed in a "reference condition" (90 kV, 3 mm Al and 0.2 mm Cu, 54.8 keV mean energy beam) but the following parameters are inserted in the sensitivity analysis: i) the beam spectrum; ii) the operators position —moving the operators to their right in direction of the patient legs (a configuration more similar to the interventional cardiology scenario in which the cardiologist works in "femoral access" condition); iii) the presence of shielding —ceiling shielding and protective goggles; iv) the beam field dimensions; v) the position of the dosemeters on the apron, shifting the scoring region from the sagittal mid-plane to the left (toward the beam) and to right (away from the beam). Quantities calculated by Monte Carlo simulations are generally given per source particle. In order to compare the outcomes with other studies a normalization is necessary. In interventional practices (and this happens also for the measurements) it is straight to express the results normalized by the KAP-meter. This is the reason why the KAP-meter has been simulated as described above.

These cases were distributed among the members of the group that use different Monte Carlo codes and version: MCNP4B [31], MCNPX [32], MCNP6 [33], PENELOPE [34] and different photon libraries (mcplib22, mcplib84, EPDL97). To improve the statistic of some results (particularly for the eye lens tally regions that have less than 1 cm^3 volumes) a variation reduction technique [35], consisting in a semi-deterministic estimator (DXTRAN sphere, in MCNP syntax), has been applied.

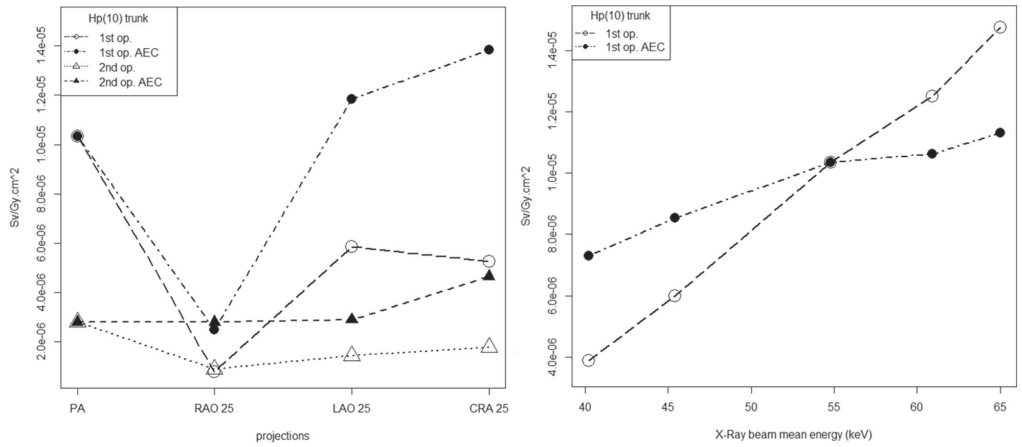

Fig. 2. – Left: simulated $H_p(10)$ for the considered beam projections at reference beam quality; Right: simulated X-ray beam qualities —70 kV, 80 kV, 90 kV reference beam, 110 kV and 100 kV— for the PA projection. (AEC means that the curve was corrected simulating the AEC effect.)

3. – Results

The simulations and the subsequent sensitivity analysis are still in progress. In this paragraph only some preliminary results are provided. The associated uncertainties are generally of the order of few per cent and always lower than 10%.

3˙1. *Simulated* $H_p(10)$. – In fig. 2, left, the simulated $H_p(10)$ values for the four considered projection, calculated for the scoring region on the trunk, on the apron at breast level, for the first and second operators are shown. The plots are normalized by the simulated KAP value. The AEC exposure correction factor is evaluated as the ratio between the given projection IDEK (Image Device Entrance Kerma) and the PA IDEK. Due to the fact that in the PA projection the patient thickness traversed by the radiation is the smallest, in all the cases the IDEK correction factor is higher than one. For the first operator, that is closest to the X-ray source, the projection plays a leading role and, as expected, the more protected condition corresponds to the RAO 25, when the image device contributes to an additional shielding for the operator upper part. This effect is not visible in the second operator, that is farther from the source, and that presents almost constant values except for the CRA 25. The data are generated for the "reference beam" (90 kV, 3 mm Al and 0.2 mm Cu, 54.8 keV mean energy beam) and, considering PA, $H_p(10)$ is about $10\,\mu$ Sv/(Gy $\cdot$ cm^2) for the first operator and and $3\,\mu$ Sv /(Gy $\cdot$ cm^2) for the second.

Generally the thicker the patient is, the higher kV is needed to compensate the lack of photon fluence in the image device. In this case, not changing the patient thickness, the "mitigation effect" of the AEC, calculated through IDEK ratios, can be clearly perceived in fig. 2, right. Here the operator-1 data for PA projection are reported as a function of the mean energy of the X-ray filtered beam spectrum, for some tested X-ray beam qualities. The $H_p(10)$ simulated values increase with the increase of the beam mean energy because of the increase of the fluence and average energy of the scattered photons toward the scoring region. This trend is consistent with the measurements

performed by Vano (for pediatric cardiology) and reported in [36]. Because the $\frac{H_p(10)}{\phi}$ conversion coefficients are monotonically increasing in the range 40–60 keV, an increase of the scattered photon average energy produces and increase of the evaluated $H_p(10)$.

In order to check the reliability of the calculated results a first comparison has been done with the literature data taken from Olgar *et al.* [37]. In that study interventional radiology procedures were considered and the X-ray data set-up (91 kV and 2.7 mm Al) is similar to that chosen as the reference condition in our work. To calculate $H_p(10)$ from the $10\,\mu\mathrm{Sv}/(\mathrm{Gy}\cdot\mathrm{cm}^2)$ and $3\,\mu\mathrm{Sv}/(\mathrm{Gy}\cdot\mathrm{cm}^2)$ rates, the median KAP values reported for PTC in table 3 by Olgar *et al.* was used. But $H_p(10)$ cannot be directly compared to the effective dose reported by Olgar *et al.* (calculated through the Niklason algorithm that uses shielded and unshielded dosemeters). For that reason we employed the thyroid unshielded dosemeter value, reported in Olgar *et al.* in table 5. This is correct because thyroid and eye lens doses are comparable in this irradiation scenario [24]. That value, 0.363 mGy, expressed in terms of absorbed dose (kerma), was converted in $H_p(10)$ using the ratio between $H_p(10)$ and kerma, 1.46, derived from our simulation, that gives 0.53 mSv.

A second comparison has been done with the measurement performed in Saint James Hospital in the interventional radiology room in the framework of a WG-12 organized study on the reliability of Active Personal Dosemeter (APD), whose results are still under revision. APD (EPD MK-2 Thermo© in this case) have been distributed to medical staff to be worn on apron in association with a passive dosemeter, a Radio Photo Luminescent (RPL) dosemeter supplied by IRSN (to be used as reference dosemeter). For different days of practice, when the doses registered by APD reached a fixed value, they were saved, reset to zero, and the associated RPL removed and substituted with a not irradiated one. These measurements were repeated and the calculated mean results per procedure ranged between 50 and 140 μSv (more details will be provided when the full analysis will be completed).

The results of these comparisons are reported in table I. Because the 1st and 2nd operators exchange their roles during the working day a "mean operator" can be considered. In that case the 0.64 mSv resulting from the simulations is consistent with the thyroid value by Olgar *et al.* (converted in $H_p(10)$) and with the data measured in Saint James Hospital. In the last case one has to take into account that it was not an *ad hoc* test performed in hospital, like in [37], but a routine monitoring with all the possible sources of influence (type of procedure different from PTC, duration, KAP values, changing roles, usage of the shielding, etc...). Comparing all this with the "rigidity" of the simulated scenario, the results can be considered satisfying.

3˙2. *Eye lens absorbed dose.* – In fig. 3, left, the simulated doses to the lens of the eyes (normalized to the simulated KAP-meter value), for the two operators, for the reference radiation and the four projections considered are reported. As in the previopus case, the RAO projection offers a further protection of the operators reducing doses to the eye lenses, on the contrary LAO increases the exposure to the operators' head. This is in agreement with what was already found in previous works [8, 9, 20]. As can be seen, for the first operator the left and right lenses doses are almost the same. This happens because it is positioned in correspondence of the beam axis (see fig. 1); instead for the second operator the known difference between the eyes is visible. In fig. 3, right, the PA eye lens doses for the two operators are shown as a function of the distance from the reference position. In these simulations the operators were shifted to the right, towards the patients legs, in a configuration that resembles, at least for the first operator, the

TABLE I. – *Calculated $H_p(10)$ per procedure and comparison with data taken from* [37] *and average of APD measurements in Saint James Hospital.*

KAP [37] values table 3 $\left(\frac{\text{microSv}}{\text{Gy}\cdot\text{cm}^2}\right)$	1st-operator dosemeter $H_p(10)$ (mSv)	2nd-operator dosemeter $H_p(10)$ (mSv)	"mean-operator" dosemeter $H_p(10)$ (mSv)	Thyroid dosemeter $H_p(10)$ [37] (mSv)	S. James Hospital $H_p(10)$ (mSv)
97.53*	1.01	0.27	0.64	0.53***	
3.95–282.55**	0.04–2.92	0.01–0.79	0.03–1.86		0.05–0.14

*Median value.
**Min and max values.
***See the text.

condition of interventional cardiology femoral access and, at the highest distance, the "conventional" factor of about two between left and right the eye lens doses [9, 38] are indeed recovered.

4. – Conclusions

WG-12 EURADOS activities are driven to radiation protection in the medical field. The present work aims at a better knowledge of the personnel radiation exposure in interventional radiology. Because the study is still in progress, the main scheme, that is based on a detailed modelling of the different aspects that characterize the medical-staff irradiation scenario, has been given with some very preliminary results which are provided for the $H_p(10)$ and for eye lens absorbed dose evaluation. The agreement between the present work outcomes and the published data can be considered a validation of the employed models. More results, including dose to the brain, effective dose and comparison with double dosimetry algorithms, are expected in the next months and a

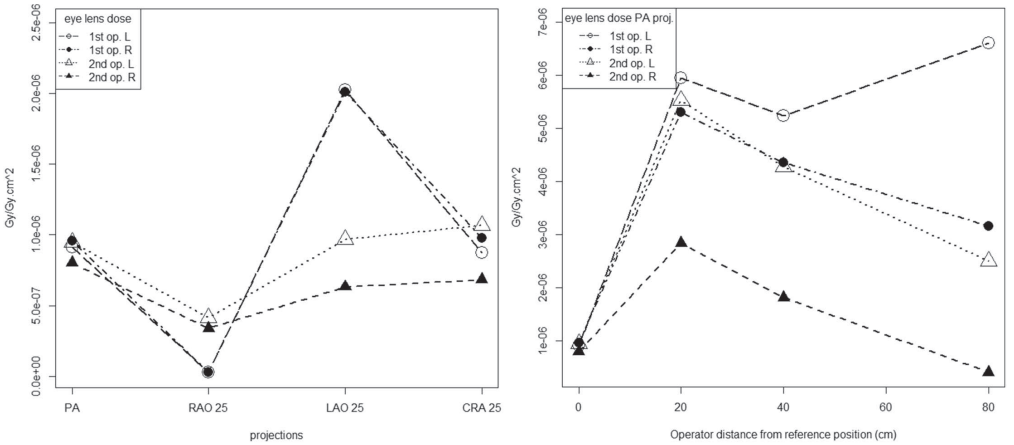

Fig. 3. – Left: absorbed doses in the eye lens per KAP; Right: Absorbed doses in the eye lens per KAP as a function of the operator distance from the X-ray beam axis —for the PA projection. (L = left eye, R = right eye)

sensitivity study though to overcome the intrinsic rigidity of the model (changing energies, position, adding shielding, etc...) will be performed with the objective of extending the information available for interventional radiology. Moreover, further measurements in hospital, employing APD, that could supply important values that could be directly compared with the Monte Carlo results, and could give a personalized feedback to the operator emphasizing the effectiveness of a specific training in radiation protection, are foreseen in the next future.

* * *

This work was supported by the European Radiation Dosimetry Group (EURADOS, WG12).

REFERENCES

[1] Vano E., Gonzales L., Guibelalde E., Fernandez J. M. and Ten J., *Br. J. Radiol.*, **71** (1998) 954.
[2] Vano E., Gonzalez L., Fernandez J. M. and Haskal Z. J., *Radiol.*, **248** (2008) 945.
[3] Vano E., Sanchez J. M. and Fernandez J. M., *Radiat. Prot. Dosim.*, **165** (2015) 235.
[4] Carinou E., Ginjaume M., O'Connor U., Kopec R. and Sans Merce M., *Radiat. Prot. Dosim.*, **165** (2015) 235.
[5] Kicken P. J., Kemerink G. J., Schultz F. W., Zotelief J., Broerse J. J. and van Engelshoven J. M. A., *Radiat. Prot. Dosim.*, **82** (1999) 105.
[6] Martin C. J., *Radiat. Prot. Dosim.*, **136** (2009) 140.
[7] Sutton D. G. and Williams J. R., *Br. J. Radiol.*, **7** (2012) 74.
[8] Koukorava C., Carinou E., Ferrari P., Krim S. and Struelens L., *Radiat. Meas.*, **46** (2011) 1216.
[9] Principi S., Farah J., Ferrari P., Carinou E., Clairand I. and Ginjaume M., *Phys. Med.*, **32** (2016) 1111.
[10] Koukorava C., Farah J., Struelens L., Clairand I., Donadille L., Vanhavere F. and Dimitriou P., *J. Radiol. Prot.*, **34** (2014) 509.
[11] Vaño E., Rosenstein M., Liniecki J., Rehani M., Martin C. J., Vetter R. J., *Recommendations of the International Commission on Radiological Protection*, edited by Clement C. H., ICRP Publication 113, *Ann. ICRP*, **39(5)**.
[12] Sailer A. M., Vergoossen L., Paulis L., van Zwam W. H., Das M., Wildeberger J. E. and Jeuken C. R. L. P. N., *Cardiov. Interv. Radiol.*, **40** (2017) 1756.
[13] Kopeć R., Novák L., Carinou E., Clairand I., Dabin J., Datz H., De Angelis C., Farah J., Huet C., Knežević Ž., Järvinen H., Majer M., Malchair F., Negri A., Haruz Waschitz S., Siiskonen T., Szumska A., Trianni A. and Vanhavere F., *Radiat. Meas.*, **71** (2014) 282.
[14] Farah J., Trianni A., Carinou E., Ciraj-Bjelac O., Clairand I., Dabin J., De Angelis C., Domienik J., Jarvinen H., Kopec R., Majer M., Malchair F., Negri A., Novak L., Siiskonen T., Vanhavere F. and Knežević Ž., *Radiat. Prot. Dosim.*, **164** (2015) 138.
[15] Farah J., Trianni A., Clairand I., Ciraj-Bjelac O., De Angelis C., Delle Canne S., Hadid L., Huet C., Jarvinen H., Negri A., Novak L., Pinto M., Siiskonen T., Waryn M. J. and Knežević Ž., *Med. Phys.*, **42** (2015) 4211.
[16] Carinou E., Ginjaume M., O'Connor U., Kopec R. and Sans Merce M., *J. Radiol. Prot.*, **34** (2014) 729.
[17] Carinou E., Ferrari P., Ciraj Bjelac O., Gingaume M., Sans Merce M. and O'Connor U., *J. Radiol. Prot.*, **35** (2015) R17.
[18] Clairand I., Ginjaume M., Vanhavere F., Carinou E., Daures J., Denozière M., Honorio da S. E., Roig M., Principi S. and Van Ryckeghem L., *Radiat. Prot. Dosim.*, **170** (2016) 21.

[19] Ciraj-Bjelac O., Carinou E., Ferrari P., Ginjaume M., Sans Merce M. and O'Connor U., *J. Am. Coll Radiol.*, **13** (2016) 1347.
[20] Ferrari P., Becker F., Carinou E., Chumak V., Farah J., Jovanovic Z., Krstic D., Morgun A., Principi S. and Telese P., *J. Radiol. Prot.*, **36** (2016) 902.
[21] Teles P., Nikodemová D., Bakhanova E., Becker F., Knežević Ž., Pereira M. F. and Sarmento S., *Radiat. Prot. Dosim.*, **174** (2017) 518.
[22] Stewart F. A., Akleyev A. V., Hauer-Jensen M., Hendry J. H., Kleiman N. J., MacVittie T. J., Aleman B. M., Edgar A. B., Mabuchi K., Muirhead C. R., Shore R. E., Wallace W. H., *Statement on Tissue Reactions/Early and Late Effects of Radiation in Normal Tissues and Organs*, edited by Clement C. H., ICRP Publication 118, *Ann. ICRP*, **41(1-2)**.
[23] Shore R. E., Neriishi K. and Nakashima E., *Radiat. Res.*, **174** (2010) 889.
[24] Kim K. P., Miller D. L., de Gonzalez A. B., Balter S., Kleinerman, Ruth A., Ostroumova E., Simon S. L. and Linet M., *Health Phys.*, **103** (2012) 80.
[25] Omar A., Kadesjö N., Palmgren C., Marteinsdottir M., Segerdahl T. and Fransson A., *J. Radiol. Prot.*, **37** (2017) 145.
[26] Snyder W. S., Ford M. R. and Warner G. G., *Nm/MIRD Panphlet N. 5* (1978).
[27] ICRP, *Report of the Task Group on Reference Man*, ICRP Publication 23 (Pergamon Press, Oxford, UK) 1975.
[28] White D. R., Griffith R. V. and Wilson I. J. (Editors), *International Commission on Radiation Units and Measurements, Photon, Electron, Proton and Neutron Interaction Data for Body Tissue ICRU Rep.* No. 46 (1992).
[29] *Catalogue of Diagnostic X ray and other Spectra IPEM*, *IPEM Sci. Rep. Ser.*, **78** (1997).
[30] *Conversion Coefficients for use in Radiological Protection against External Radiation*, *ICRU Rep.*, **57** (1996).
[31] Briesmeister J. F. (Editor), *MCNPTM - A General Monte Carlo N-Particle Transport Code*, Version 4B LA-12625-M (1997).
[32] Pelowitz D. B. (Editor), *2005 MCNPX User's manual*, LA-CP-05-0369 (2005).
[33] Pelowitz D. B. (Editor), *2013 MCNP6 User's Manual* version 1.0 LA-CP-13-00634 (2013).
[34] Salvat F., Fernandez-Varea J. M., Sempau J., *A Code System for Monte Carlo Simulation of Electron and Photon Transport - Workshop Barcelona NEA/NSC/DOC*, 2015.
[35] Gualdrini G. and Ferrari P., *Radiat. Prot. Dosim.*, **146** (2011) 425.
[36] Vano E., Ubeda C., Leyton F., Miranda P. and Gonzales L., *Pediatr. Cardiol.*, **30** (2009) 409.
[37] Olgar T., Bor D., Berkmen G. and Yazar T., *J. Radiol. Prot.*, **29** (2009) 393.
[38] Higgins A., *J. Radiol. Prot.*, **36** (2016) 74.